Author Manuscript

Author Manuscript

Author Manuscript

Author Manuscript

HHS Public Access

Author manuscript

Mol Cancer Ther. Author manuscript; available in PMC 2020 September 01.

Published in final edited form as:

Mol Cancer Ther. 2020 March ; 19(3): 731–741. doi:10.1158/1535-7163.MCT-19-0809.

Targeting protein translation by rocaglamide and didesmethylrocaglamide to treat MPNST and other sarcomas

Long-Sheng Chang[1,2,3,4,*], **Janet L. Oblinger**[1,2], **Sarah S. Burns**[1,2], **Jie Huang**[1,2], **Larry W. Anderson**[5], **Melinda G. Hollingshead**[5], **Rulong Shen**[4], **Li Pan**[6], **Garima Agarwal**[6], **Yulin Ren**[6], **Ryan D. Roberts**[1,2], **Barry R. O'Keefe**[5,7], **A. Douglas Kinghorn**[6], **Jerry M. Collins**[5]

[1]Center for Childhood Cancer and Blood Diseases, Abigail Wexner Research Institute, Nationwide Children's Hospital, Columbus, OH 43205, USA

[2]Department of Pediatrics, The Ohio State University College of Medicine, Columbus, OH 43210, USA

[3]Department of Otolaryngology-Head & Neck Surgery,The Ohio State University College of Medicine, Columbus, OH 43210, USA

[4]Department of Pathology, The Ohio State University College of Medicine, Columbus, OH 43210, USA

[5]Department of Division of Cancer Treatment and Diagnosis, Center for Cancer Research, National Cancer Institute, NIH, Frederick, MD 21702, USA

[6]Department of Division of Medicinal Chemistry and Pharmacognosy, The Ohio State University College of Pharmacy, Columbus, OH 43210, USA

[7]Department of Molecular Targets Program, Center for Cancer Research, National Cancer Institute, NIH, Frederick, MD 21702, USA

Abstract

Malignant peripheral nerve sheath tumors (MPNSTs) frequently overexpress eIF4F components, and the eIF4A inhibitor silvestrol potently suppresses MPNST growth. However, silvestrol has suboptimal drug-like properties, including a bulky structure, poor oral bioavailability (<2%), sensitivity to MDR1 efflux, and pulmonary toxicity in dogs. We compared 10 silvestrol-related rocaglates lacking the dioxanyl ring and found that didesmethylrocaglamide (DDR) and rocaglamide (Roc) had growth-inhibitory activity comparable to silvestrol. Structure-activity

*Corresponding author: Long-Sheng Chang, Center for Childhood Cancer and Blood Diseases, Abigail Wexner Research Institute at Nationwide Children's Hospital, 700 Children's Drive, Columbus, OH 43205, USA; Phone: 614-355-2658; Fax: 614-722-5895, Long-Sheng.Chang@nationwidechildrens.org.

Authors' Contributions

Conception and design: LSC, JLO, SSB, LWA, MGH, ADK, and JMC

Development of Methodology: LSC, JLO, SSB, JH, LWA, MGH

Acquisition of data: LSC, JLO, SSB, JH, LWA, MGH, RS, GA

Analysis and interpretation of data: LSC, JLO, SSB, LWA, ADK, JMC

Writing, review, and/or revision of the manuscript: LSC and JLO wrote the initial draft and all authors reviewed the manuscript

Administrative, technical, or material support: LSC, JLO, SSB, RR, LP, YR, BRO, ADK, JMC

Study Supervision: LSC, ADK, and JMC

Disclosure of Potential Conflicts of Interest

No potential conflicts of interest were disclosed.

Author Manuscript Author Manuscript Author Manuscript Author Manuscript

relationship analysis revealed that the dioxanyl ring present in silvestrol was dispensable for, but may enhance, cytotoxicity. Both DDR and Roc arrested MPNST cells at G_2/M, increased the sub-G_1 population, induced cleavage of caspases and poly(ADP-ribose) polymerase, and elevated the levels of the DNA-damage response marker γH2A.X, while decreasing the expression of AKT and ERK1/2, consistent with translation inhibition. Unlike silvestrol, DDR and Roc were not sensitive to MDR1 inhibition. Pharmacokinetic analysis confirmed that Roc had 50% oral bioavailability. Importantly, Roc, when administered intraperitoneally or orally, showed potent anti-tumor effects in an orthotopic MPNST mouse model and did not induce pulmonary toxicity in dogs as found with silvestrol. Treated tumors displayed degenerative changes and had more cleaved caspase-3-positive cells, indicative of increased apoptosis. Furthermore, Roc effectively suppressed the growth of osteosarcoma, Ewing sarcoma, and rhabdomyosarcoma cells and patient-derived xenografts. Both Roc- and DDR-treated sarcoma cells showed decreased levels of multiple oncogenic kinases, including IGF-1R. The more favorable drug-like properties of DDR and Roc and the potent anti-tumor activity of Roc suggest that these rocaglamides could become viable treatments for MPNST and other sarcomas.

Precis

Rocaglamide and didesmethylrocaglamide exhibit better drug-like properties than silvestrol and possess potent anti-tumor activity in multiple types of sarcomas

Keywords

Rocaglamide (Roc); didesmethylrocaglamide (DDR); malignant peripheral nerve sheath tumor (MPNST); Ewing sarcoma; osteosarcoma; rhabdomyosarcoma; orthotopic; cell line-derived xenograft (CDX); patient-derived xenograft (PDX); bioluminescence imaging (BLI)

Introduction

Malignant peripheral nerve sheath tumors (MPNSTs) are characterized as aggressive soft-tissue sarcomas with a high risk of recurrence and metastasis. Often refractory to current treatment, these tumors have a poor five-year survival rate of only about 20~50% (1). Therefore, development of more effective medical therapy that eradicate MPNSTs is of significant clinical need. MPNSTs can occur sporadically or arise from pre-existing plexiform neurofibromas in patients with neurofibromatosis type 1 (NF1), a tumor predisposition syndrome caused by mutations in the *NF1* gene which encodes the Ras-GTPase-activating protein neurofibromin. Importantly, even sporadic tumors frequently harbor mutations in the *NF1* gene or the Ras pathway. Consequently, both sporadic and NF1-associated MPNSTs exhibit upregulation of Ras downstream kinase signaling, including the phosphatidylinositol 3-kinase (PI3K)-AKT-mammalian target of rapamycin (mTOR) and Raf-MEK-ERK mitogen-activated protein kinases. MPNSTs also exhibit overexpression or aberrant activation of epidermal growth factor receptor (EGFR), platelet-derived growth factor receptor (PDGFR), and insulin-like growth factor-1 receptor (IGF-1R) (2,3). These reports suggest that these Ras downstream kinases and deregulated receptor tyrosine kinases (RTKs) may be therapeutic targets. Additionally, recurrent mutations in the tumor suppressor genes *CDKN2A* and *TP53* and the subunits of the chromatin-modifying

Author Manuscript Author Manuscript Author Manuscript Author Manuscript

polycomb repressor complex-2 (PRC2), *SUZ12* and *EED*, have been identified and are important for MPNST progression (4). Inactivation of *CDKN2A* and *TP53* disables the G_1/S checkpoint. The loss of PRC2 function can lead to enhanced Ras-driven gene transcription (5).

As MPNSTs often exhibit hyperactive Ras activity, statins and farnesyl transferase inhibitors, which prevent localization of Ras to the membrane and inhibit MPNST cell growth (6,7), have been evaluated but do not improve survival in patients with advanced cancer (8–10). Drugs that target the deregulated RTKs and mitogenic kinases have also been investigated in patients with MPNSTs; however, the results have so far been disappointing. The EGFR inhibitor erlotinib elicited poor response rates in MPNSTs with only one of 20 patients exhibiting stable disease (11). The IGF-1R blocking antibodies, such as ganitumab, show limited objective single-agent activity (12). Sorafenib, which inhibits Raf and several RTKs, has only minimal activity in patients with sarcomas (13). The mTOR inhibitor rapamycin and its derivatives, such as everolimus, cause cytostatic responses and are being evaluated in combination with other targeted drugs. However, a recent trial showed that combination of everolimus with bevacizumab, a monoclonal antibody that binds vascular endothelial growth factor (VEGF) and prevents activation of the RTK VEGF receptor, was not effective in patients with refractory MPNSTs (14). A phase II study is ongoing to evaluate the dual mTOR complexes 1 and 2 inhibitor TAK-228 in soft-tissue sarcomas (https://clinicaltrials.gov Identifier:). Collectively, the modest and transient patient responses from the completed trials indicate that targeting more than one critical pathway is likely needed to achieve a cure.

To sustain uncontrolled growth, cancer cells commonly exhibit enhanced protein translation by upregulation of the translation machinery (15). The most highly regulated step in the protein biosynthetic pathway occurs during translation initiation, in which the eukaryotic initiation factor 4F (eIF4F) complex is recruited to the 5’ untranslated region (5’-UTR) of mRNA. This complex is composed of three subunits: eIF4G, a scaffolding protein; eIF4E, a cap-binding protein, and eIF4A, an RNA helicase which unwinds the secondary structure of the 5’-UTR. We have shown over-expression of the three eIF4F components in multiple types of human cancer, including MPNST (16,17). Genetic inhibition of eIF4A and eIF4E using short-hairpin RNAs reduces MPNST cell proliferation. In addition, the pro-survival and pro-growth activities of several signaling pathways, such as PI3K-AKT-mTOR and Raf-MEK-ERK frequently activated in human cancer, occur in part by facilitating eIF4F-mediated translation initiation. The mTOR kinase phosphorylates and inactivates the eIF4E-binding protein (4E-BP) translational repressors (18). Both AKT and ERKs phosphorylate eIF4B, which then associates with and increases the helicase activity of eIF4A (19). Moreover, AKT, mTOR, and the downstream ERK1/2 kinase p90 ribosomal S6 kinase can phosphorylate and inactivate an endogenous repressor of eIF4A activity, the programmed cell death 4 (PDCD4) protein. Further, the mRNAs that depend upon eIF4A for efficient translation usually contain long 5’-UTRs with guanine-rich sequences termed G-quadruplexes which can form four-stranded structures with G-tetrads stacked on one another (15). These eIF4A-dependent transcripts are often found in genes encoding oncoproteins, transcription factors associated with super enhancers, epigenetic regulators, and kinases (20). Interestingly, we found that the eIF4A inhibitor silvestrol suppresses MPNST cell

Author Manuscript Author Manuscript Author Manuscript Author Manuscript

growth at low nanomolar of $IC_{50,}$ decreases the levels of multiple mitogenic kinases including AKT and ERKs, and profoundly impairs the growth of MPNST xenografts (16). These results suggest that direct targeting of the translation initiation components, particularly eIF4A, might be an effective treatment strategy for these tumors.

Silvestrol is part of a large family of compounds termed flavaglines or rocaglates, which share a cyclopenta[*b*]benzofuran structure (21,22). It possesses potent antitumor activity in multiple other cancer models (23–25). However, silvestrol has some suboptimal drug-like properties. It is relatively large with a bulky dioxanyl ring, making the total synthesis of silvestrol laborious (26–28). It is a substrate for the multidrug resistance 1 (MDR1) transporter (29) and has very limited oral bioavailability of <2% (30).

To search for compounds with better drug-like properties, we analyzed ten rocaglates that lack the dioxanyl moiety and examined the structure-activity relationships for this compound class. We showed that two of these compounds, rocaglamide (Roc) and didesmethylrocaglamide (DDR), exhibited potent growth inhibitory activity with IC_{50} values comparable to silvestrol. Importantly, these rocaglamides were not sensitive to MDR1 inhibition and Roc exhibited oral bioavailability and potent anti-tumor effects against multiple types of sarcomas.

Methods

Natural Compounds

Ten silvestrol-related rocaglates, inclusive of (−)-didesmethylrocaglamide, were isolated from the tropical plant *Aglaia perviridis*, collected in Vietnam as part of a multi-institutional collaborative project on the discovery of new antineoplastic natural compounds. The full structures and absolute configurations of these rocaglates were determined (31). For *in vitro* studies, purified silvestrol and related rocaglates were dissolved as a 10-mM stock in dimethyl sulfoxide (DMSO; Sigma-Aldrich). A 60-mg sample of (−)-rocaglamide (NSC326408) was prepared at the U.S. National Cancer Institute for *in vivo* studies.

Cell Lines, Cell Proliferation Assays, and Flow Cytometry

Various MPNST, Ewing sarcoma, osteosarcoma, rhabdomyosarcoma, schwannoma, meningioma, and leukemia cell lines used in this study are described in Supplementary Methods. All cell lines were authenticated by Short tandem repeat genotyping and tested to be mycoplasma-free. Cell proliferation was assessed using resazurin assays and cell cycle analysis was performed as previously described (32).

Western Blots

Subconfluent cells were treated with the indicated doses of Roc or DDR for 1–3 days and lysed. Equal amounts of protein lysates were analyzed by immunoblotting. Detailed procedures and the antibodies used are described in Supplementary Methods.

Author Manuscript Author Manuscript Author Manuscript Author Manuscript

Pharmacokinetic (PK) analysis

Mice were administered with a 5mg/kg dose of Roc by intravenous (IV) or intraperitoneal injection (IP) or by oral gavage (PO). Blood samples were collected before and at multiple time-points after dosing (n=3). Plasma concentrations of Roc were analyzed using a sensitive liquid chromatography coupled with tandem mass spectrometry (LC/MS-MS) (Supplementary Methods).

Cell Line-Derived Xenograft (CDX) and Patient-Derived Xenograft (PDX) Models and In Vivo Efficacy

All animal work was performed according to the protocols approved by the Institutional Animal Care and Use Committee at Nationwide Children's Hospital. For animal dosing, Roc was formulated in 30% hydroxypropyl-β-cyclodextrin (HPβCD). The quantifiable, orthotopic MPNST CDX model was generated as described previously (33). Mice bearing established ST8814-Luc tumors (16) were randomized into three groups (n=10/group) and treated with the predetermined maximum tolerated dose (MTD) of Roc at 4mg/kg by IP or 1.2mg/kg by oral gavage, or the vehicle HPβCD every other day. Tumor growth was measured weekly by BLI.

To generate PDX models, the Nationwide Children's Hospital Institutional Review Board approved the Human Subjects Protocol. After obtaining informed written consents from the subjects, tumor specimens were used to establish PDX models. Mice with actively-growing PDX tumors for a Ewing sarcoma (NCH-EWS-2), an osteosarcoma (NCH-OS-7), and an alveolar rhabdomyosarcoma (NCH-ARMS-2) reaching ~100–200 mm^3 were randomized into two treatment groups (n=10/group) for each PDX model and treated with 3mg/kg of Roc or HPβCD by IP every other day, followed by tumor measurement twice weekly (Supplementary Methods).

Immunohistochemistry

Sections from Roc or vehicle-treated MPNST tumors were prepared and stained with hematoxylin and eosin (H&E) or immunostained for p-histone H3(Ser^{10}) (pH3; ab32107, Abcam) or CC3 (#9664, Cell Signaling) as previously described (32).

Results

DDR and Roc possess potent growth-inhibitory activity comparable to silvestrol

To search for compounds with better drug-like properties, we side-by-side compared ten rocaglates lacking the dioxanyl ring (31) with silvestrol for growth-inhibitory activity in a panel of MPNST, schwannoma, and meningioma cell lines, which we previously showed to be sensitive to the antiproliferative action of silvestrol (16,17). We found that several of these rocaglates maintained potent growth inhibition comparable to silvestrol. In particular, the IC_{50} values of Roc were slightly higher than silvestrol, while DDR reliably demonstrated ~2-fold more potent than silvestrol in all cell lines tested (Fig. 1, Table 1, and Supplementary Fig. S1), indicating that the dioxanyl moiety is dispensable for cytotoxicity. Further structure-activity comparison discerned some positions on the cyclopenta[*b*]benzofuran scaffold that affected the antiproliferative activity of rocaglates.

Author Manuscript Author Manuscript Author Manuscript Author Manuscript

Similar to previous observations, the substitution of a methoxy group at position 8b, as in 8b-*O*-methylrocaglaol versus rocaglaol, abolished the activity (Fig. 1). This methoxy substitution at 8b could be partly mitigated by the addition of a methylenedioxy ring to phenyl ring B. Additionally, the presence of amide or ester groups at position C-2 of the benzofuran scaffold appeared to enhance the activity, as compounds such as DDR, Roc, and methyl rocaglate were more potent than rocaglaol. Since the amide group at the C-2 position confers superior growth inhibition, we further evaluated DDR and Roc for their mechanisms of action.

Rocaglamides induce G_2/M arrest and cell death

Flow cytometry analysis revealed that human *NF1*-expressing STS26T and *NF1*-null ST8814 MPNST cells treated with one- or two-IC_{50} doses of DDR or Roc for three days exhibited a marked increase in the G_2/M fraction (Supplementary Fig. S2A and S2B). The sub-G_1 fraction, suggestive of apoptosis, was noticeably prominent in treated STS26T cells, especially at the two-IC_{50} dose (Supplementary Fig. S2A). Phase contrast micrographs taken of cells prior to cell cycle analysis showed increased floating dead cells and debris in DDR or Roc-treated dishes. While ST8814 cells treated for three days did not show obvious signs of cell death (Supplementary Fig. S2B), a six-day incubation resulted in increased numbers of floating dead cells with a commensurate expansion of the sub-G_1 fraction (Supplementary Fig. S2C). Collectively, these results indicate that, like silvestrol (16), DDR and Roc inhibit MPNST cell proliferation by inducing cell cycle arrest at G_2/M and subsequently, cell death.

DDR and Roc increase caspase and PARP cleavage and activate the DNA damage response, while suppressing mitogenic signaling pathways

To confirm induction of apoptosis in rocaglamide-treated MPNST cells, we analyzed protein expression of several markers important for this process. STS26T cells treated for 3 days with either DDR or Roc exhibited increased cleavage of the executioner caspases-3 and 7 and their downstream substrate PARP (Fig. 2A). A concomitant decrease in the amounts of intact caspases 3 and 7 and PARP was observed, consistent with the enhanced cleavage of these apoptotic markers and possibly due to direct effects of these rocaglamides on protein translation. Likewise, the levels of the pro-survival kinases AKT and ERK1/2 were diminished in rocaglamide-treated MPNST cells. Importantly, treatment with rocaglamides also resulted in higher levels of the DNA damage response marker γH2A.X. This increase occurred as early as one day after DDR treatment before the occurrence of cell death (Fig. 2B). Similarly, cleavage of caspase-3 and PARP and induction of γH2A.X were also detected in *NF1*-null ST8814 cells treated with DDR and Roc (Supplementary Fig. S3). These results demonstrate that DDR and Roc induce apoptosis in both *NF1*-expressing and *NF1*-deficient MPNST cells, possibly subsequent to the activation of the DNA damage response.

Rocaglamides are not sensitive to MDR1 inhibition and Roc is orally bioavailable

The MDR1/P-glycoprotein (Pgp) encoded by the *ABCB1* (ATP-binding cassette subfamily B member 1) gene is implicated in limiting the bioavailability of several chemotherapeutics and confers drug resistance in tumors that overexpress this protein. Silvestrol is a substrate of MDR1/Pgp, which may be related to its poor oral bioavailability (29,30). To determine

Author Manuscript Author Manuscript Author Manuscript Author Manuscript

whether there are any differences in the sensitivity to MDR1/Pgp between rocaglamides and silvestrol, we treated silvestrol-resistant 697-R leukemic cells, which overexpress MDR1/Pgp (Supplementary Fig. S4), and the parental silvestrol-sensitive 697 cells with various concentrations of each compound. Similar to previous findings (29), we found that 697-R cells were less sensitive to silvestrol inhibition than 697 cells (26 vs 3.5nM of $IC_{50,}$ respectively; Fig. 3A). Surprisingly, DDR- and Roc-treated 697-R cells exhibited IC_{50} values very similar to those of parental 697 cells (4 vs 3nM of $IC_{50,}$ respectively, for DDR and 15 vs 8nM of $IC_{50,}$ respectively, for Roc; Figs. 3B and 3C). Also, we observed that various MPNST cell lines expressed different levels of MDR1 protein (Supplementary Fig. S4). For example, ST8814 cells expressed a higher level of MDR1 than STS26T cells. Curiously, both cell lines showed similar sensitivity to growth inhibition by DDR and Roc (Table 1 and Supplementary Fig. S1). Together, these results indicate that these rocaglamides are no longer sensitive to MDR1 inhibition.

To examine the oral bioavailability, we conducted PK studies to compare mice that had been dosed with Roc at 5mg/kg via the IV, IP, or PO route, followed by measuring Roc concentrations in blood samples collected at various times post dosing. Two separate studies with three mice at each time point for each dosing route were conducted. The maximum mean observed concentration (C_{max}) reached ~11μM for the IV route, ~4μM for the IP route, and ~0.8μM for the PO route (Fig. 4A). Areas under the plasma concentration-time curves (AUC_{0-7h}) produced 245μM*min of exposure in the IV route and 142μM*min of exposure in the PO route. The concentrations of Roc appeared to decline more slowly in the plasma over 24h ($T_{½}$=2.4h) with the PO route compared to those dosed by the IV route ($T_{½}$=1.5h). Based on the estimation from AUC_{0-7h}, Roc exhibited ~50% oral bioavailability, confirming improved bioavailability of Roc over silvestrol.

Roc, when administered intraperitoneally or orally, exhibits potent anti-tumor effects in an orthotopic MPNST model

To evaluate the *in vivo* activity of Roc, we treated NSG mice bearing luciferase-expressing ST8814-Luc tumors implanted in the sciatic nerve with Roc at the predetermined MTD (4mg/kg by IP or 1.2mg/kg orally), or HPβCD vehicle every other day. As shown in Figs. 4B/4C, tumor bioluminescence from vehicle-treated mice steadily and rapidly increased by >10,000-fold over four-week treatment. In contrast, tumor bioluminescence from mice treated with Roc by IP only increased by an average of <10-fold, showing >99% reduction in tumor luminescence compared to controls. Similarly, Roc, when administered orally, also exhibited potent tumor inhibition with bioluminescence decreasing by >95%. In addition, we did not observe any significant changes in body weight of animals treated with the indicated doses of Roc, compared with vehicle-treated controls (Supplementary Fig. S5).

Histological analysis revealed that while MPNSTs treated with HPβCD vehicle for four weeks had large nuclei with prominent nucleoli and displayed active mitotic figures (Fig. 4D, top left panel), tumors treated with Roc by IP had pleomorphic nuclei with abundant foamy cytoplasm resembling histiocytoid degenerative changes (top middle panel). A few enlarged tumor cells with multinucleated appearance and scattered apoptosis were present. Degenerative changes and cell death were also observed in tumors treated with orally-

Author Manuscript Author Manuscript Author Manuscript Author Manuscript

delivered Roc (top right panel). Consistent with G_2/M arrest, tumor cells treated with IP- or orally-delivered Roc exhibited much higher prevalence of phospho-histone H3 labeling compared to vehicle-treated tumors (middle panels). In addition, Roc-treated tumors displayed increased numbers of cleaved caspase-3 positive cells which often coincided with those with multinucleated-like appearance (bottom panels). Taken together, these results indicate that Roc has oral bioavailability and possesses potent *in vivo* efficacy against MPNSTs.

Roc and DDR have broad antitumor activity against common types of pediatric sarcoma

Since MPNSTs comprise only ~2% of all sarcomas (34), we expanded our testing of Roc and DDR to three other types of sarcomas more prevalent seen in children and young adults: Ewing sarcoma, osteosarcoma, and rhabdomyosarcoma. Using a series of commonly-used cell lines, including two Ewing sarcoma cell lines (A673 and TC32), four osteosarcoma cell lines (143B, MG-63, Saos2, and OS17), and one rhabdomyosarcoma cell line (RD), we showed that, as in MPNST cells, both rocaglamides were highly active against all of these sarcoma cell lines (Supplementary Figs. S6A–C). Also, we observed that DDR consistently exhibited lower IC_{50} values than Roc in every sarcoma cell line tested.

Subsequently, we evaluated the *in vivo* activity of Roc using PDX models for a Ewing sarcoma, an osteosarcoma, and an alveolar rhabdomyosarcoma. We discovered that Roc was highly potent in suppressing the growth of Ewing sarcoma PDXs and inhibited tumor growth by an average of ~90% over four-week treatment (Fig. 5A). Similarly, the average size of Roc-treated osteosarcoma PDX tumors was reduced by ~80% compared to those of vehicle-treated tumors (Fig. 5B). Also, Roc inhibited the growth of rhabdomyosarcoma PDXs by ~70% (Fig. 5C). Notably, the volumes of tumors in individual Roc-treated mice showed very little overlap with those in vehicle-treated mice, particularly for the Ewing sarcoma and osteosarcoma PDX models (Fig. 5). Together with the findings from the MPNST model, these results demonstrate that Roc displays significant antitumor effects against multiple types of sarcoma.

Rocaglamides decrease multiple signaling kinases and transcription factors important for sarcoma cell growth

To further examine the molecular mechanisms underlying the antiproliferative effects of rocaglamides, we treated TC32 Ewing sarcoma, 143B osteosarcoma, and RD rhabdomyosarcoma cells with one- or two-IC_{50} dose of DDR or Roc for 1–2 days followed by Western blotting for several known drivers of cell survival and proliferation. Interestingly, we found that these rocaglamides reliably reduced the levels of the β subunit of IGF-1R, an upstream activator of PI3K-AKT signaling, in all three sarcoma cell lines (Figs. 6A–C). We also observed reduction of the IGF-1Rβ levels in rocaglamide-treated MPNST cells (Supplementary Fig. S7). In addition, both rocaglamides decreased the levels of AKT, ERKs, cyclin D1 and survivin in treated TC32, 143B, and RD cells (Fig. 6). Intriguingly, the oncogenic fusion protein EWS-FLI1, which act as an aberrant transcription factor in Ewing sarcoma (35), was not affected in Roc- and DDR-treated TC32 Ewing sarcoma cells (Fig. 6A). Consistent with this observation, these rocaglamides did not inhibit EWS expression in 143B osteosarcoma and RD rhabdomyosarcoma cells (Figs. 6B/C). However, the levels of

Author Manuscript Author Manuscript Author Manuscript Author Manuscript

lysine demethylase 1 (LSD1), which modulates EWS-FLI1 transcriptional activity (36), and NKX2.2, an EWS-FL11-regulated gene necessary for oncogenic transformation (37), were diminished by these rocaglamides in TC32 cells (Fig. 6A). Collectively, these results suggest that rocaglamides potently suppress sarcoma growth by decreasing multiple key signaling proteins important for tumor growth and survival.

Comparative toxicology studies in canines show that Roc does not induce pulmonary toxicity found with silvestrol

As the next part of the standard process for developing compounds as candidates for human evaluation, a toxicology study in dogs was conducted through a contractor of the NCI Experimental Therapeutics program. Unexpectedly, silvestrol was found to cause massive lung damage, while Roc did not produce adverse pulmonary findings when tested on the same protocol at the same lab. Further details are contained in the online summary reports for both silvestrol and Roc at: https://dtp.cancer.gov/publications/silvestrol_rocaglamide_studies.pdf.

Discussion

For decades, treatments for MPNSTs and other sarcomas have remained largely unchanged with current standard of care combining surgical resection with intensive multi-agent chemotherapy (1,34,38,39). Radiation may be used depending upon the tumor type and clinical presentation. While this multidisciplinary treatment strategy may help local control, it is not effective for metastatic and recurrent disease. Also, these multimodal regimens are associated with considerable acute and long-term toxicities that impact patients' quality of life. Despite recent advances in understanding tumor biology and targeted therapy development, an FDA-approved medical therapy for the treatment of these malignancies is still not available. We previously showed that eIF4A is a vulnerable point of disruption in MPNSTs and that the eIF4A inhibitor silvestrol potently suppresses MPNST growth (16). Regretfully, silvestrol exhibited an unexpected pulmonary toxicity in dogs and its further development as a cancer therapy was suspended (DM Lucas, MA Phelps, AD Kinghorn, M Grever, in preparation). We have identified two rocaglates lacking the dioxanyl ring, Roc and DDR, with better drug-like properties than silvestrol and possessing antitumor efficacy in multiple sarcoma models, including MPNST. Most critically, Roc did not induce the toxicity found in dogs with silvestrol under the same conditions.

Our side-by-side comparison of 10 rocaglates lacking the bulky dioxanyl ring present in silvestrol has allowed us to discern certain structure-activity relationships, particularly the C-8b, C-2, and C-6 positions along the cyclopenta[*b*]benzofuran core. Consistent with previous reports (22,40), the hydroxy group at the C-8b position is essential for antiproliferative activity. This finding is consistent with the crystal structure of Roc complexed with eIF4A and polypurine RNA, which reveals hydrogen bonding between the 8b-OH of Roc and a guanine base in the RNA (41). Also, the phenyl rings A and B of Roc parallel stack with RNA bases, which may explain our finding that adding a methylenedioxy group to ring B modestly improved the growth inhibitory activity of rocaglates with methylated 8b-OH (Fig. 1). It is possible that this methylenedioxy ring may enhance the

Author Manuscript Author Manuscript Author Manuscript Author Manuscript

affinity of the rocaglates to the eIF4A-RNA complex, partially compensating for the loss of 8b hydrogen bonding.

Among the rocaglates lacking the dioxanyl ring that we evaluated, DDR was the most potent, suggestive of the importance of having a simple primary amide group at the C-2 position. While the presence of a dioxanyl ring instead of a methoxy group at the C-6 position enhances the potency of silvestrol compared with methyl rocaglate (22,42), our data indicated that this ring is not required for cytotoxicity. However, it appears to play an important role in MDR1-induced resistance as Roc and DDR are no longer susceptible to this inhibitory effect. Consistent with this notion, we detected a higher level of MDR1 in ST8814 MPNST cells than that in STS26T cells (Supplementary Fig. S4), while the IC_{50} values of Roc and DDR in ST8814 cells were similar to those in STS26T cells (Table 1 and Supplementary Fig. S1). The MDR1 transporter binds to silvestrol and is thought to limit its oral bioavailability (29). Our PK analysis demonstrating 50% oral bioavailability of Roc, a >25-fold improvement over silvestrol, confirms this prediction and strongly suggests a possible interaction of MDR1 with the dioxanyl moiety. The observed oral bioavailability of Roc allows a greater flexibility for dosing. More importantly, we found that Roc, when administered intraperitoneally or orally, showed potent anti-tumor effects in an orthotopic MPNST CDX mouse model and effectively suppressed the growth of PDX models for Ewing sarcoma, osteosarcoma, and rhabdomyosarcoma.

Like silvestrol, rocaglamides exert their potent growth-inhibitory and antitumor activities mainly through inhibition of eIF4A and protein translation (43,44). Consistently, we observed that Roc and DDR decreased the levels of multiple signaling proteins important for tumor growth and survival, leading to G_2/M cell cycle arrest and activation of executioner caspases. In addition to AKT and ERKs, rocaglamides reduced the levels of IGF-1R in all sarcoma cell lines tested. This decrease in IGF-1R expression, coupled with the simultaneous inhibition of AKT and ERKs, likely results in superior inhibition of IGF-1 signaling compared to the simple blockade at the receptor level. Our results further suggest that IGF-1R may serve as a biomarker for responsiveness to rocaglamides in sarcomas.

It should be noted that the effects of translation inhibition mediated by eIF4A are different from those by eIF4E, which can be activated by the AKT/mTOR pathway, a commonly deregulated event in sarcomas (18). The mTOR inhibitor, rapamycin and its analogs, and mTOR kinase inhibitors only cause cytostatic effects and tumor stabilization (45). Also, blocking mTOR signaling is associated with activation of bypass signaling pathways that can restore critical survival signals, enabling tumor regrowth. Inhibition of eIF4E tends to decrease translation of the mRNAs with 5’ terminal oligopyrimidine tracts, which encode ribosomal proteins, elongation factors, lysosomal-related and metabolic-related proteins. However, the eIF4A activity is more critical in unwinding the mRNAs with long 5’-UTRs that can form G-quadruplexes, such as *AKT* and *IGF-1R* (15,20). In addition, some transcripts, e.g., *c-MYC*, are translated from internal ribosomal entry sites that do not require the cap binder eIF4E and are insensitive to eIF4E inhibition (46). Thus, blocking eIF4A may have a stronger effect on tumor growth and survival.

Author Manuscript Author Manuscript Author Manuscript Author Manuscript

Ewing sarcoma is frequently driven by the chimeric fusion oncogene *EWS-FLI1* due to a chromosomal translocation that fuses an RNA-binding protein, EWSR1, with the FLI1 transcription factor (35). Surprisingly, we found that the levels of EWS-FLI1 remained unchanged in rocaglamide-treated Ewing sarcoma cells (Fig. 6A). As a ubiquitously expressed protein, the EWSR1 levels were also not affected in other types of sarcoma cells treated with rocaglamides (Figs. 6B/C). In contrast, the levels of the epigenetic modulator LSD1, a protein needed for optimal activity of the EWS-FLI1 transcriptional complex (36), and a key EWS-FLI1 downstream target NKX2.2, a homeobox transcription factor implicated in development (37), were diminished by DDR and Roc treatment (Fig. 6). Upon inspection of these genes, we noted that the *EWSR1* transcript has a very short 5'-UTR, while the mRNAs for *NKX2.2* and *LSD1/KDM1A* contain longer G+C-rich 5'-UTRs. Therefore, we hypothesize that the *NKX2.2* and *LSD1/KDM1A* transcripts are eIF4A-dependent.

Intriguingly, prior to caspase activation, rocaglamide-treated MPNST cells exhibited increased γH2A.X, suggesting that DNA damage may be a key underlying cause of the apoptosis seen at later time points. Rocaglamides may affect prohibitin-mediated ERK activation, cause the disruption of mitochondrial integrity, and/or promote the generation of reactive oxygen species (47,48). Alternatively, they may affect translation of the proteins responsible for DNA replication and repair, resulting in stalled replication forks or inadequate repair of DNA damage. We are presently examining these possibilities.

Roc was the first member of the cyclopenta[*b*]benzofuran class identified as a novel antileukemic agent from *Aglaia elliptifolia* by King et al. (49). It is worth mentioning that the structures of Roc and DDR are simpler than silvestrol; therefore, they should be more amenable to chemical synthesis (50). As DDR exhibited higher *in vitro* potency against various types of sarcoma cells than Roc, we anticipate that DDR will have superior anti-tumor efficacy. Experiments are in progress to compare these rocaglamides in various sarcoma animal models.

In summary, we have demonstrated that Roc and DDR, as eIF4A inhibitors, simultaneously suppressed multiple growth-promoting signaling pathways and induced apoptosis in tumor cells. Roc was no longer sensitive to MDR1 inhibition. It was orally bioavailable and exhibited potent anti-tumor effects in multiple sarcoma models with no overt toxicity. These promising results indicate that these rocaglamides merit further investigation as treatments for patients with MPNSTs and other sarcomas.

Supplementary Material

Refer to Web version on PubMed Central for supplementary material.

Acknowledgments

We thank Melissa Sammons of NCH Tumor Core for assistance with PDX models, Eva Majerova for technical help with plasma analysis, John Byrd for 697 and 697-R cells, Stephen Lessnick for Ewing sarcoma cells, and Ruoning Wang for rhabdomyosarcoma cells.

Grant Support

Author Manuscript Author Manuscript Author Manuscript Author Manuscript

This study was supported by grants from CancerFree KIDS, Sunbeam Foundation, and Department of Defense (W81XWH-16-1-0104 and W81XWH-18-1-0547 to LSC), National Cancer Institute (P01CA125066 to ADK and P30CA16058 to The OSU Comprehensive Cancer Center), and NCI Experimental Therapeutics program (NCI Contract HHSN261200800001 to Leidos Biomedical Research).

References

1. Kim A, Stewart DR, Reilly KM, Viskochil D, Miettinen MM, Widemann BC. Malignant Peripheral Nerve Sheath Tumors State of the Science: Leveraging Clinical and Biological Insights into Effective Therapies. Sarcoma. 2017;2017:7429697. [PubMed: 28592921]
2. Perrone F, Da Riva L, Orsenigo M, Losa M, Jocollè G, Millefanti C, et al. PDGFRA, PDGFRB, EGFR, and downstream signaling activation in malignant peripheral nerve sheath tumor. Neuro Oncol. 2009;11:725–736. [PubMed: 19246520]
3. Yang J, Ylipää A, Sun Y, Zheng H, Chen K, Nykter M, et al. Genomic and molecular characterization of malignant peripheral nerve sheath tumor identifies the IGF1R pathway as a primary target for treatment. Clin Cancer Res. 2011;17(24):7563–73. [PubMed: 22042973]
4. Kim A, Pratilas CA. The promise of signal transduction in genetically driven sarcomas of the nerve. Exp Neurol. 2018;299(Pt B):317–325. [PubMed: 28859862]
5. De Raedt T, Beert E, Pasmant E, Luscan A, Brems H, Ortonne N, et al. PRC2 loss amplifies Ras-driven transcription and confers sensitivity to BRD4-based therapies. Nature. 2014;514:247–51. [PubMed: 25119042]
6. Sebti SM, Tkalcevic GT, Jani JP. Lovastatin, a cholesterol biosynthesis inhibitor, inhibits the growth of human H-ras oncogene transformed cells in nude mice. Cancer Commun. 1991;3:141–147. [PubMed: 2043425]
7. Barkan B, Starinsky S, Friedman E, Stein R, Kloog Y. The Ras inhibitor farnesylthiosalicylic acid as a potential therapy for neurofibromatosis type 1. Clin Cancer Res. 2006;12:5533–5542. [PubMed: 17000690]
8. Rao S, Cunningham D, de Gramont A, Scheithauer W, Smakal M, Humblet Y, et al. Phase III double-blind placebo-controlled study of farnesyl transferase inhibitor R115777 in patients with refractory advanced colorectal cancer. J Clin Oncol. 2004;22:3950–3957. [PubMed: 15459217]
9. Cloughesy TF, Wen PY, Robins HI, Chang SM, Groves MD, Fink KL, et al. Phase II trial of tipifarnib in patients with recurrent malignant glioma either receiving or not receiving enzyme-inducing antiepileptic drugs: a North American Brain Tumor Consortium Study. J Clin Oncol. 2006;24:3651–3656. [PubMed: 16877733]
10. Hanrahan EO, Kies MS, Glisson BS, Khuri FR, Feng L, Tran HT, et al. A phase II study of Lonafarnib (SCH66336) in patients with chemorefractory, advanced squamous cell carcinoma of the head and neck. Am J Clin Oncol. 2009;3:274–279.
11. Albritton KH, Rankin C, Coffin CM, Ratner N, Budd GT, Schuetze SM, et al. Phase II study of erlotinib in metastatic or unresectable malignant peripheral nerve sheath tumors (MPNST). J Clin Oncol. 2006;24:18(suppl): 9518–9518.
12. Tap WD, Demetri G, Barnette P, Desai J, Kavan P, Tozer R, et al. Phase II study of ganitumab, a fully human anti-type-1 insulin-like growth factor receptor antibody, in patients with metastatic Ewing family tumors or desmoplastic small round cell tumors. J Clin Oncol. 2012;30:1849–1856. [PubMed: 22508822]
13. Maki RG, D'Adamo DR, Keohan ML, Saulle M, Schuetze SM, Undevia SD, et al. Phase II study of sorafenib in patients with metastatic or recurrent sarcomas. J Clin Oncol. 2009;27:3133–3140. [PubMed: 19451436]
14. Widemann BC, Meyer CF, Cote GM, Chugh R, Milhem MM, Van Tine BA, et al. SARC016: phase II study of everolimus in combination with bevacizumab in sporadic and neurofibromatosis type 1 (NF1) related refractory malignant peripheral nerve sheath tumors (MPNST). J Clin Oncol. 2016;34(15_suppl):11053–11053.
15. Malka-Mahieu H, Newman M, Désaubry L, Robert C, Vagner S. Molecular Pathways: The eIF4F Translation Initiation Complex-New Opportunities for Cancer Treatment. Clin Cancer Res. 2017;23:21–25. [PubMed: 27789529]

Author Manuscript Author Manuscript Author Manuscript Author Manuscript

16. Oblinger JL, Burns SS, Akhmametyeva EM, Huang J, Pan L, Ren Y, et al. Components of the eIF4F complex are potential therapeutic targets for malignant peripheral nerve sheath tumors and vestibular schwannomas. Neuro-Oncol. 2016;18:1265–1277. [PubMed: 26951381]
17. Oblinger JL, Burns SS, Huang J, Pan L, Ren Y, Shen R, et al. Overexpression of eIF4F components in meningiomas and suppression of meningioma cell growth by inhibiting translation initiation. Exp Neurol. 2018;299(Pt B):299–307. [PubMed: 28610844]
18. Mamane Y, Petroulakis E, LeBacquer O, Sonenberg N. mTOR, translation initiation and cancer. Oncogene. 2006;25:6416–6422. [PubMed: 17041626]
19. Chu J, Cargnello M, Topisirovic I, Pelletier J. Translation initiation factors: reprogramming protein synthesis in cancer. Trends Cell Biol. 2016;26:918–933. [PubMed: 27426745]
20. Wolfe AL, Singh K, Zhong Y, Drewe P, Rajasekhar VK, Sanghvi VR, et al. RNA G-quadruplexes cause eIF4A-dependent oncogene translation in cancer. Nature. 2014;513:65–70. [PubMed: 25079319]
21. Pan L, Woodard JL, Lucas DM, Fuchs JR, Kinghorn, AD. Rocaglamide, silvestrol, and related bioactive compounds from *Aglaia* species. Nat Prod Rep. 2014:31;924–931. [PubMed: 24788392]
22. Kinghorn AD, DE Blanco EJ, Lucas DM, Rakotondraibe HL, Orjala J, Soejarto DD, et al. Discovery of anticancer agents of diverse natural origin. Anticancer Res. 2016;36:5623–5637. [PubMed: 27793884]
23. Lucas DM, Edwards RB, Lozanski G, West DA, Shin JD, Vargo MA, et al. The novel plant-derived agent silvestrol has B-cell selective activity in chronic lymphocytic leukemia and acute lymphoblastic leukemia *in vitro* and *in vivo*. Blood. 2009;113:4656–4666. [PubMed: 19190247]
24. Kogure T, Kinghorn AD, Yan I, Bolon B, Lucas DM, Grever MR, Patel T. Therapeutic potential of the translation inhibitor silvestrol in hepatocellular cancer. PLoS One. 2013;8:e76136. [PubMed: 24086701]
25. Boussemart L, Malka-Mahieu H, Girault I, Allard D, Hemmingsson O, Tomasic G, et al. eIF4F is a nexus of resistance to anti-BRAF and anti-MEK cancer therapies. Nature. 2014;513:105–109. [PubMed: 25079330]
26. El Sous M, Khoo ML, Holloway G, Owen D, Scammells PJ, Rizzacasa MA. Total synthesis of (−)-episilvestrol and (−)-silvestrol. Angew Chem Int Ed Engl. 2007;46:7835–7838. [PubMed: 17823902]
27. Gerard B, Cencic R, Pelletier J, Porco JA Jr. Enantioselective synthesis of the complex rocaglate (−)-silvestrol. Angew Chem Int Ed Engl. 2007;46:7831–7834. [PubMed: 17806093]
28. Adams TE, El Sous M, Hawkins BC, Hirner S, Holloway G, Khoo ML, et al. Total synthesis of the potent anticancer Aglaia metabolites (−)-silvestrol and (−)-episilvestrol and the active analogue (−)-4'-desmethoxyepisilvestrol. J Am Chem Soc. 2009;131:1607–1616. [PubMed: 19140688]
29. Gupta SV, Sass EJ, Davis ME, Edwards RB, Lozanski G, Heerema NA, et al. Resistance to the translation initiation inhibitor silvestrol is mediated by ABCB1/P-glycoprotein overexpression in acute lymphoblastic leukemia cells. AAPS J. 2011;13:357–364. [PubMed: 21538216]
30. Saradhi UV, Gupta SV, Chiu M, Wang J, Ling Y, Liu Z, et al. Characterization of silvestrol pharmacokinetics in mice using liquid chromatography-tandem mass spectrometry. AAPS J. 2011;13:347–56. [PubMed: 21499689]
31. Pan L, Acuña UM, Li J, Jena N, Ninh TN, Pannell CM, et al. Bioactive flavaglines and other constituents isolated from *Aglaia perviridis*. J Nat Prod. 2013;76:394–404. [PubMed: 23301897]
32. Burns SS, Akhmametyeva EM, Oblinger JL, Bush ML, Huang J, Senner V, et al. Histone deacetylase inhibitor AR-42 differentially affects cell-cycle transit in meningeal and meningioma cells, potently inhibiting NF2-deficient meningioma growth. Cancer Res. 2013;73:792–803. [PubMed: 23151902]
33. Burns SS, Chang L-S. Generation of noninvasive, quantifiable, orthotopic animal models for NF2-associated schwannoma and meningioma. Methods Mol Biol. 2016;1427:59–72 [PubMed: 27259921]
34. Farid M1, Demicco EG, Garcia R, Ahn L, Merola PR, Cioffi A, Maki RG. Malignant peripheral nerve sheath tumors. Oncologist. 2014;19:193–201. [PubMed: 24470531]

Author Manuscript Author Manuscript Author Manuscript Author Manuscript

35. Delattre O, Zucman J, Plougastel B, Desmaze C, Melot T, Peter M, et al. Gene fusion with an ETS DNA-binding domain caused by chromosome translocation in human tumours. Nature. 1992;359:162–165. [PubMed: 1522903]
36. Sankar S, Bell R, Stephens B, Zhuo R, Sharma S, Bearss DJ, Lessnick SL. Mechanism and relevance of EWS/FLI-mediated transcriptional repression in Ewing sarcoma. Oncogene. 2013;32:5089–5100. [PubMed: 23178492]
37. Smith R, Owen LA, Trem DJ, Wong JS, Whangbo JS, Golub TR, Lessnick SL. Expression profiling of EWS/FLI identifies NKX2.2 as a critical target gene in Ewing's sarcoma. Cancer Cell. 2006;9:405–416. [PubMed: 16697960]
38. Brown HK, Schiavone K, Gouin F, Heymann MF, Heymann D. Biology of Bone Sarcomas and New Therapeutic Developments. Calcif Tissue Int. 2018;102(2):174–195. [PubMed: 29238848]
39. Skapek SX, Ferrari A, Gupta AA, Lupo PJ, Butler E, Shipley J, et al. Rhabdomyosarcoma. Nat Rev Dis Primers. 2019;5:1. [PubMed: 30617281]
40. Ebada SS, Lajkiewicz N, Porco JA Jr, Li-Weber M, Proksch P. Chemistry and biology of rocaglamides (= flavaglines) and related derivatives from Aglaia species (Meliaceae). Prog Chem Org Nat Prod. 2011;94:1–58. [PubMed: 21833837]
41. Iwasaki S, Iwasaki W, Takahashi M, Sakamoto A, Watanabe C, Shichino Y, et al. The translation inhibitor rocaglamide targets a bimolecular cavity between eIF4A and polypurine RNA. Mol Cell. 2019;73:738–748. [PubMed: 30595437]
42. Kim S, Salim AA, Swanson SM, Kinghorn AD. Potential of cyclopenta[*b*]benzofurans from Aglaia species in cancer chemotherapy. Anticancer Agents Med Chem. 2006;6:319–345. [PubMed: 16842234]
43. Cencic R, Carrier M, Galicia-Vázquez G, Bordeleau ME, Sukarieh R, Bourdeau A, et al. Antitumor activity and mechanism of action of the cyclopenta[b]benzofuran, silvestrol. PLoS One. 2009;4:e5223. [PubMed: 19401772]
44. Sadlish H, Galicia-Vazquez G, Paris CG, Aust T, Bhullar B, Chang L, et al. Evidence for a functionally relevant rocaglamide binding site on the eIF4A-RNA complex. ACS Chem Biol. 2013;8:1519–1527. [PubMed: 23614532]
45. D'Abronzo LS, Ghosh PM. eIF4E phosphorylation in prostate cancer. Neoplasia. 2018;20:563–573. [PubMed: 29730477]
46. Wiegering A, Uthe FW, Jamieson T, Ruoss Y, Hüttenrauch M, Küspert M, et al. Targeting translation initiation bypasses signaling crosstalk mechanisms that maintain high MYC levels in colorectal cancer. Cancer Discov. 2015;5:768–781. [PubMed: 25934076]
47. Polier G, Neumann J, Thuaud F, Ribeiro N, Gelhaus C, Schmidt H, et al. The natural anticancer compounds rocaglamides inhibit the Raf-MEK-ERK pathway by targeting prohibitin 1 and 2. Chem Biol. 2012;19:1093–1104. [PubMed: 22999878]
48. Callahan KP, Minhajuddin M, Corbett C, Lagadinou ED, Rossi RM, Grose V, et al. Flavaglines target primitive leukemia cells and enhance anti-leukemia drug activity. Leukemia. 2014;28:1960–1968. [PubMed: 24577530]
49. King ML, Chiang CC, Ling HC, Fujita E, Ochiai M, McPhail AT. X-ray crystal structure of rocaglamide, a novel antileukemic 1*H*-cyclopenta[*b*]benzofuran from *Aglaia elliptifolia*. J Chem Soc, Chem Commun. 1982;20:1150–1151.
50. Liu T, Nair SJ, Lescarbeau A, Belani J, Peluso S, Conley J, et al. Synthetic silvestrol analogues as potent and selective protein synthesis inhibitors. J Med Chem. 2012;55:8859–8878. [PubMed: 23025805]

Author Manuscript Author Manuscript Author Manuscript Author Manuscript

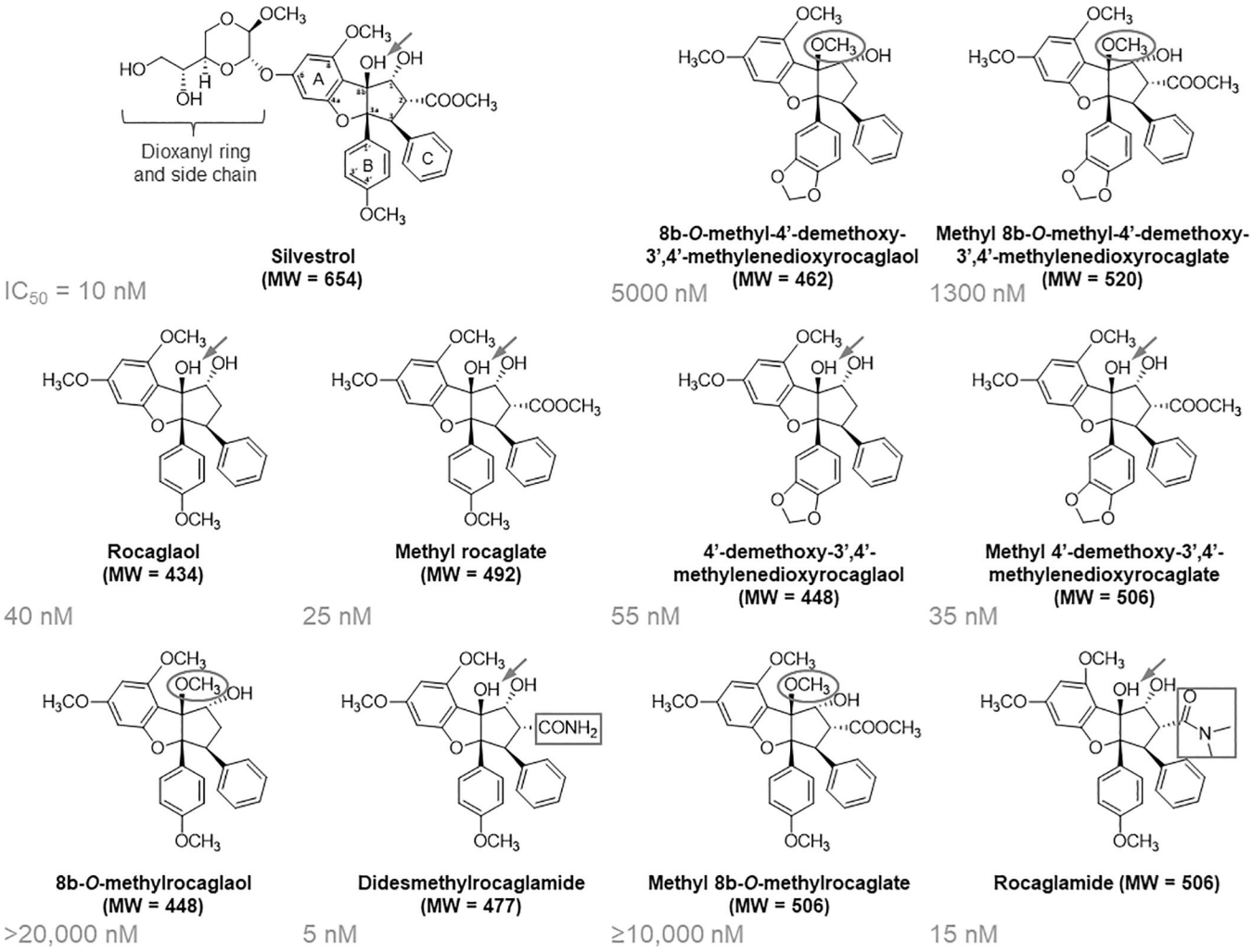

Figure 1. Identification of didesmethylrocaglamide and rocaglamide with potent growth-inhibitory activity comparable to silvestrol.

The structure of each rocaglate is shown along with its IC_{50} value in STS26T MPNST cells as determined in Table 1. Structure-activity comparison revealed that the dioxanyl (dioxanyloxy) ring is dispensable but may enhance the cytotoxicity of rocaglates. An unmethylated C-8b hydroxyl group (arrow) and the amide functionality (rectangle) of didesmethylrocaglamide and rocaglamide are important for optimum antiproliferative activity, while methylation of the C-8b hydroxyl group (oval) substantially impaired the activity.

Author Manuscript Author Manuscript Author Manuscript Author Manuscript

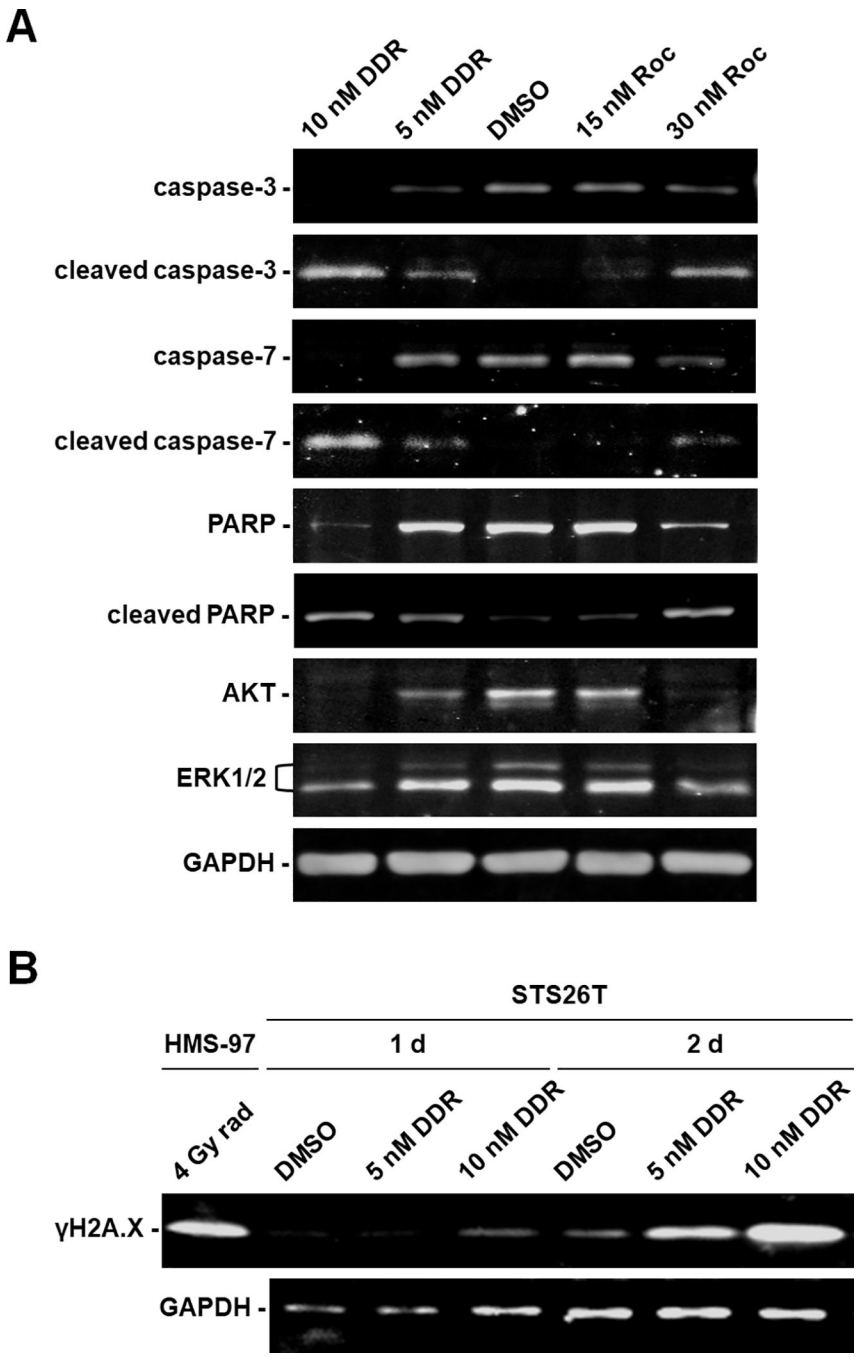

Figure 2. DDR and Roc increase caspase and PARP cleavage and elevate the levels of γH2A.X while decreasing AKT and ERK expression in MPNST cells.

(A) Protein lysates prepared from STS26T cells treated for 3 days with 1- or 2-IC_{50} of DDR or Roc were analyzed by Western blots for full-length and cleaved caspase-3/7 and PARP, as well as AKT and ERK1/2. GAPDH served as a loading control. (B) Protein lysates from STS26T cells treated for 1 and 2 days with 1- or 2-IC_{50} of DDR were probed for the expression of phosphorylated H2A.X (γH2A.X). As a positive control, lysates from HMS-97 human malignant schwannoma cells irradiated with 4 Grays (Gy) of X-ray were used.

Author Manuscript Author Manuscript Author Manuscript Author Manuscript

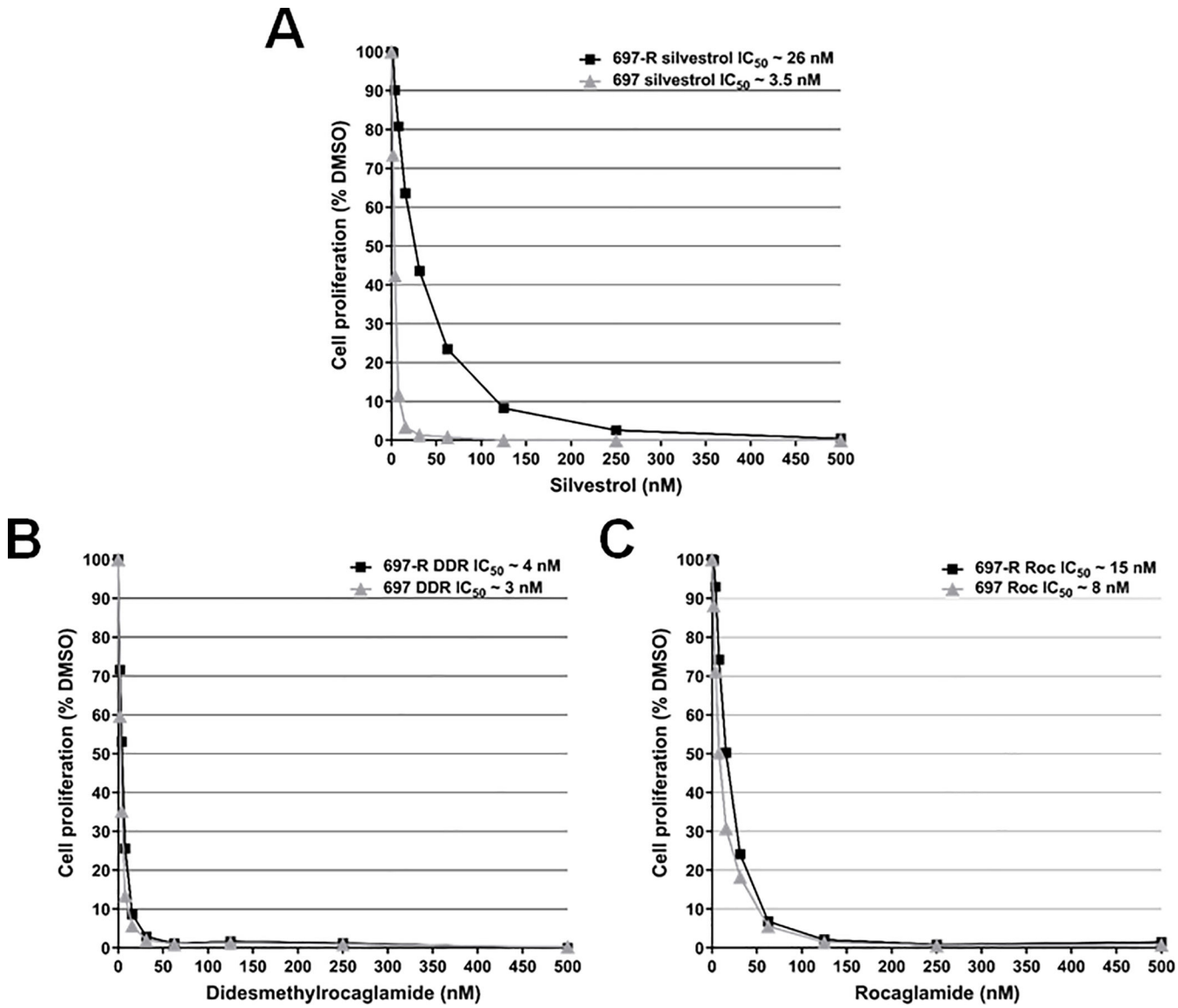

Figure 3. Unlike silvestrol, DDR and Roc inhibits proliferation of MDR1-overexpressing 697-R leukemic cells at IC_{50} values similar to parental 697 cells.

Cell proliferation was measured on 697-R and 697 cells treated for 3 days with various concentrations of silvestrol (A), DDR (B), and Roc (C). Each treatment was performed in six replicates, and each experiment was repeated twice. Shown are representative dose-response growth inhibition curves for all three drugs from experiments run in parallel. The insets show the IC_{50} values for each compound.

Author Manuscript Author Manuscript Author Manuscript Author Manuscript

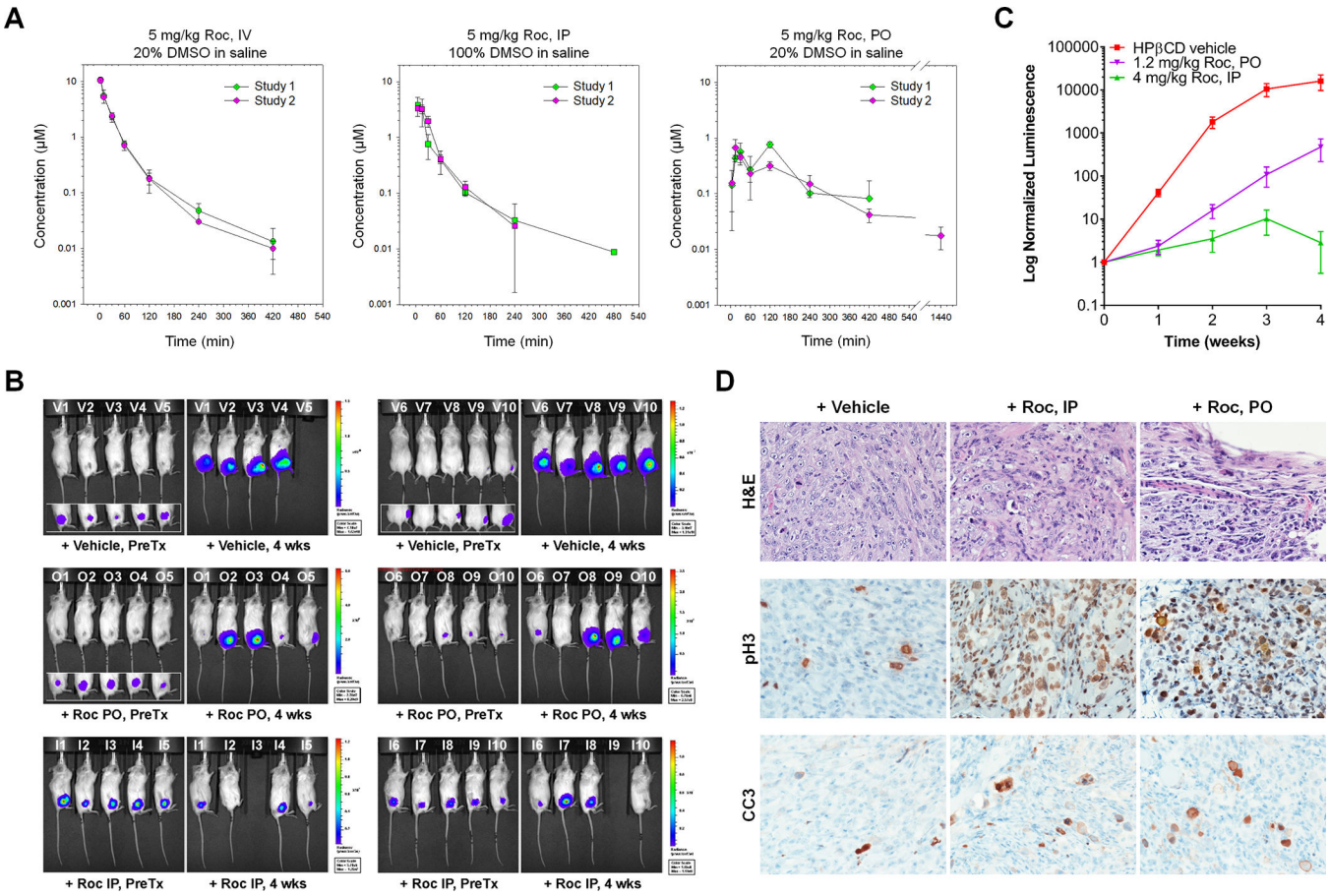

Figure 4. Roc has 50% oral bioavailability and potently suppresses the growth of orthotopic MPNST xenografts.

(A) Plasma concentration-time profiles of Roc were obtained by PK analysis according to Methods. The mean concentration of Roc with standard deviation (SD) in mouse plasma for each time point after IV, IP, and PO administration was plotted. For each dosing route, two independent studies were performed. (B) Shown are representative BL images of ST8814-Luc MPNST-bearing mice prior to (PreTx) and 4 weeks (wks) after treatment with Roc at 4mg/kg by IP, 1.2mg/kg by PO, or HPβCD vehicle every other day. (C) The relative tumor-emitted BL signals were denoted as % of total flux after treatment relative to the total flux prior to treatment designated as one (100%). The data are shown as mean ± SD. For each treatment group, at least 7 mice completed the full treatment schedule. Note that tumor bioluminescence from vehicle-treated mice rapidly increased by an average of ~17,000-fold over four weeks. However, tumor bioluminescence from the Roc IP group grow only by ~3-fold and from the Roc PO group increased ~470-fold on average. (D) H&E staining show that while vehicle-treated xenografts contained large vesicular nuclei with prominent nucleoli and mitotic activity, tumors treated with Roc by IP had pleomorphic nuclei and many enlarged tumor cells had abundant foamy cytoplasm resembling histiocytoid degenerative changes along with scattered apoptosis (top panels). Degenerative tumor cells were also present in tumors treated with orally-delivered Roc. Tumor necrosis with necrotic debris separating mostly degenerative tumor cells with viable vasculature was also observed.

Author Manuscript Author Manuscript Author Manuscript Author Manuscript

Immunostaining revealed abundant phospho-histone H3 (pH3)-labeled cells in Roc-treated tumors compared to vehicle-treated tumors (middle panels). Increased numbers of cleaved caspase-3 (CC3)-positive cells were detected in Roc-treated tumors (bottom panels).

Author Manuscript Author Manuscript Author Manuscript Author Manuscript

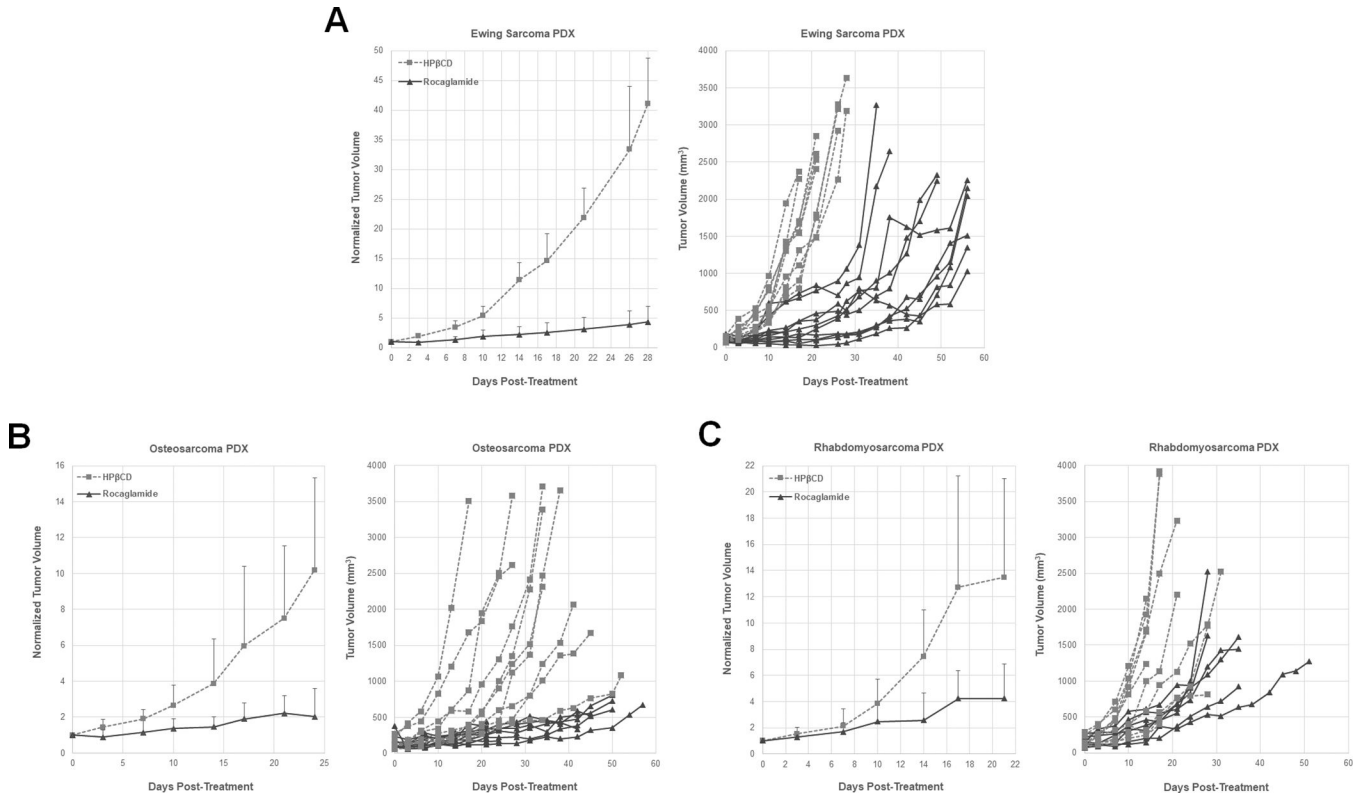

Figure 5. Roc exhibits potent anti-tumor effects in multiple sarcoma PDX models.

Mice with growing Ewing sarcoma (A), osteosarcoma (B), and rhabdomyosarcoma (C) PDXs were treated with 3mg/kg of Roc or HPβCD vehicle by IP every other day. Tumor diameters were measured twice weekly and volumes calculated according to Methods. The normalized tumor volume, denoted as the ratio of the calculated tumor volume after treatment relative to the volume prior to treatment designated as one, was plotted as the mean tumor volume of the entire treatment group at each time point with SD (A, C, and E). The calculated tumor volume for each individual mouse over time was also plotted (B, D, and F).

Author Manuscript Author Manuscript Author Manuscript Author Manuscript

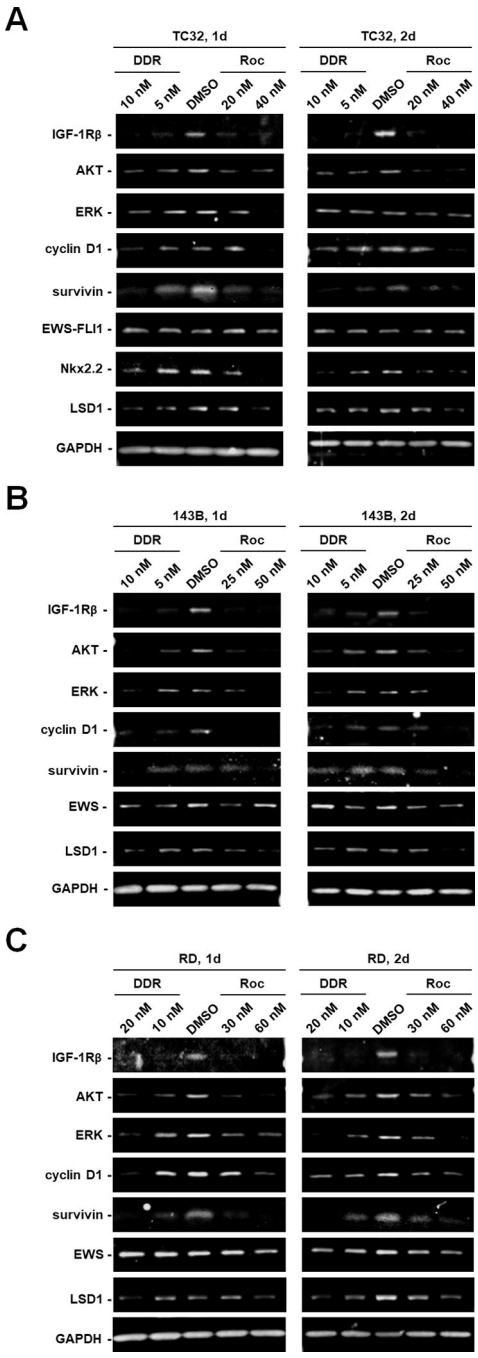

Figure 6. DDR and Roc reduce multiple signaling proteins important for sarcoma cell growth and survival.

Protein lysates from TC32 Ewing sarcoma (A), 143B osteosarcoma (B), and RD rhabdomyosarcoma (C) cells treated for 1 and 2 days with the indicated concentrations of DDR or Roc were analyzed by Western blotting for various oncogenic driver proteins. GAPDH was used as a loading control.

Author Manuscript Author Manuscript Author Manuscript Author Manuscript

Table 1.

The growth-inhibitory activity of silvestrol and 10 related rocaglates lacking the dioxanyl ring in *NF1*$^{+/+}$ STS26T and *NF1*$^{-/-}$ ST8814 MPNST, *Nf2*$^{-/-}$ schwannoma, and *NF2*$^{-/-}$ meningioma cells.

The average IC_{50} value of each rocaglate was determined by 3-day resazurin proliferation assays as described in Methods. Didesmethylrocaglamide (DDR) and rocaglamide (Roc) were found to possess growth-inhibitory activity similar to or more potent than silvestrol. ND, not determined.

Compound	MW (Da)	IC_{50} (nM)			
		Sch10545 *Nf2*$^{-/-}$ schwannoma cells	Ben-Men-1 *NF2*$^{-/-}$ meningioma cells	STS26T *NF1*$^{+/+}$ MPNST cells	ST8814 *NF1*$^{-/-}$ MPNST cells
Silvestrol	654	70	10	10	40
8b-*O*-methyl-4’-demethoxy-3’,4’-methylenedioxyrocaglaol	462	>2,500	>2,500	5,000	10,000
Methyl 8b-*O*-methyl-4’-demethoxy-3’,4’-methylenedioxyrocaglate	520	1,900	3,800	1,300	2,000
Rocaglaol	434	60	100	40	90
Methyl rocaglate	492	50	55	25	35
4’-demethoxy-3’,4’-methylenedioxyrocaglaol	448	65	85	55	120
Methyl 4’-demethoxy-3’,4’-methylenedioxyrocaglate	506	60	80	35	70
8b-*O*-methylrocaglaol	448	>20,000	>20,000	>20,000	>20,000
Didesmethylrocaglamide	477	10	5	5	5
Methyl 8b-*O*-methylrocaglate	506	9,300	>10,000	>10,000	>20,000
Rocaglamide	506	ND	15	15	20